Plasma Chem Plasma Process (2013) 33:1099–1109
DOI 10.1007/s11090-013-9479-z

ORIGINAL PAPER

Decomposition of Trimethylamine by an Electron Beam

Youn-Suk Son · Pillheon Kim · Jun Hyung Park · Junghwan Kim · Jo-Chun Kim

Received: 16 April 2013 / Accepted: 15 August 2013 / Published online: 3 September 2013

Abstract To identify the decomposition characteristics of trimethylamine (TMA) by electron beam (EB), we conducted an experiment based on process parameters, including absorbed dose (2.5–10 kGy), background gas (air, O_2, N_2 and He), water content (1,200, 14,300, and 27,500 ppm), initial concentration (50, 100, and 200 ppm) and reactor type (batch or continuous flow system). Air background gas showed a maximum TMA removal efficiency of 86 % at 10 kGy and that was the highest efficiency of all background gases. Energy efficiencies were higher when the absorbed dose was lower (e.g., 2.5 kGy). Decomposition efficiencies of all initial TMA concentrations were approximately >90 % at 10 kGy. Removal efficiencies increased up to 30 % as water vapor increased. As a by-product, it is observed that CH_3 radical formed by EB irradiation was converted into CH_4 by reaction with residual TMA, $(CH_3)_2NH$, and H. These results suggest that EB technology can be applied for TMA treatment under low concentration and high flow rate conditions.

Keywords Electron beam · Trimethylamine · By-products · Odorous compounds · CH_3 radical

Introduction

Odorous compounds are emitted from various sources and are easily detected at extremely low concentrations (below ppb levels) in ambient air because the threshold value is low

Y.-S. Son
Exposure, Epidemiology, and Risk Program, Department of Environmental Health, Harvard School of Public Health, Boston, MA, USA

Y.-S. Son · P. Kim · J. Kim · J.-C. Kim (✉)
Department of Environmental Engineering, Konkuk University, Seoul, Republic of Korea
e-mail: jckim@konkuk.ac.kr

J. H. Park
Department of Eco Friendly Research, Korea Dyeing Technology Center, Taegu, Repubic of Korea

[1]. Trimethylamine (TMA) is an odorous compound generated from dead animals, and, particularly, when fish decompose. Anthropogenic TMA is generated from diverse sites such as dye and waste water treatment facilities, livestock farms, fish processing plants, and landfills [2].

Trimethylamine can affect humans by irritating and damaging not only the eyes and respiratory organs but also the liver and spleen [3]. Thus, TMA concentrations in working environments in Korea where human exposure can be high have been set at a time-weighted average (TWA) of 10 ppm and a short-term exposure limit (STEL) of 15 ppm. Furthermore, levels set by the American Conference of Governmental Industrial Hygienists are more strict with a TWA and STEL values of 5 and 15 ppm, respectively.

Conventional technologies for removing odorous compounds include absorption, adsorption, incineration and biofiltration [4, 5]. However, these methods have disadvantages such as high operating and maintenance costs [6, 7]. Advanced technologies such as plasma, photocatalysts, and electron beam (EB) have been studied to solve these problems [8, 9]. Especially, an EB is useful for sources emitting low concentrations and high-volume flow because the reaction produces free radicals and ions in 10^{-8}–10^{-1} s [10, 11]. In addition, an EB can be operated at ambient temperature without additional equipment [12].

Most studies on removing odorous compounds using advanced technologies have focused on some compounds such as toluene, xylene, and sulfur compounds. However, no studies on TMA decomposition characteristics or removal efficiency using advanced technologies have been published.

This study was carried out to understand TMA removal efficiencies and characteristics based on process parameters, including absorbed dose, background gas, water content, initial concentration and reactor type. The by-products generated by EB irradiation were also identified.

Experimental

Batch and Flow System

An experiment was conducted in batch and continuous flow systems to study TMA removal characteristic by EB. A 1 MeV EB accelerator (maximum power 40 kW, ELV-4 type, Korea Dyeing Technology Center, Korea) was used.

First, the batch system was used to investigate basic decomposition characteristics by influencing the removal factors such as background gas, water content, and absorbed dose. The reactor used in the batch system was a 1 L Tedlar bag (SKC, Inc., USA), which is relatively stable for EB irradiation. This reactor was passed under the irradiation window of the EB accelerator at a velocity of 10 m/min via a conveyor system.

Second, a continuous flow test was performed under similar conditions to the actual site to confirm TMA removal efficiencies at initial concentrations (50–200 ppm) and absorbed doses (2.5–10 kGy). A 250 L/min volume compressor (NCP01, AM TECH, Korea) was used to supply air flow in a continuous flow control system, and silica gel, purafil, and activated charcoal scrubbers were used to remove moisture and air pollutants (VOCs, SOx, and NOx) so that zero air flowed inside the system. During this period, the retention time inside the round-shaped stainless steel reactor (70 mm diameter, 55 mm high, and 0.212 L) was 0.85 s. A TMA generator comprised of a standard gas (TMA 1 %/N_2, Rigas, Korea) and a mixing chamber were used to produce consistently low TMA concentrations (50–200 ppm).

A cellulose triacetate film dosimeter (FTR = 125, Fuji, Tokyo, Japan) was used to measure the absorbed dose in the reactors. Detailed information regarding the reactors and absorbed doses was published previously [13].

Sampling Method

Trimethylamine has a significantly low threshold value (approximately 0.032 ppb). Therefore, sampling and analysis of trace TMA gases are important. Two hard glass impingers with 20 ml sulfuric acid were used in series to absorb the TMA. The system for sampling was composed of lines, pumps, and flow meters.

The sample obtained by the impinger was analyzed using the headspace method. The sample (4 ml) was mixed with KOH solution (5 ml) in a vial and was reacted in a sonicater for 20 min. Then, TMA eluted into the gas phase of the vial was adsorbed by a solid phase microextraction fiber (SPME; polydimethylsiloxane/divinylbenzene, 65 μm, Supelco, USA) and analyzed by gas chromatography/nitrogen phosphorus detection (GC/NPD) (HP 7890 Gas Chromatograph, Hewlett Packard, USA).

Analytic Method

Gas chromatography/nitrogen phosphorus detection was used to conduct a quantitative analysis before and after EB irradiation, and DB-1 (50 m × 0.32 mm × 0.52 μm, Hewlett Packard, USA) was used in the column. The TMA was reacted at 50 °C in 2 min and adsorbed by the SPME fiber over 15 min to extract the TMA using the headspace method. The sample extracted by the SPME fiber was desorbed at 250 °C in 400 s and analyzed. The linear correlation between the injected mass and the GC/NPD response was high ($r^2 = 0.995$).

A non-dispersive infrared CO/CO_2 measuring device (Gas Data PAQ, Gas data Ltd., UK) was used to measure carbon monoxide and carbon dioxide concentrations. Moreover, an ozone analyzer (model 49C O_3 Analyzer, Thermo Electron Corp., USA) was used to measure ozone concentrations.

Results and Discussion

Background Gases

N_2, O_2, and air (99.999 %) were used as background gases to compare TMA removal efficiencies among the different background gases. Additionally, He was used to confirm only the primary electron effects excluding secondary activated species such as $OH^{\cdot}$, $HO_2^{\cdot}$, $O^{\cdot}$, and $N^{\cdot}$. Primary electrons generated by EB irradiation generally react with N_2, O_2, and H_2O as background gases to form radicals, ions, and secondary electrons [10, 11, 14, 15]. Ranges of the absorbed doses were adjusted to 2.5–10 kGy. Figure 1 shows the TMS (200 ppm) removal efficiencies depending on the background gas. The relative standard deviation values of duplicated samples using the GC/NPD were <10 %.

The TMA residual ratio (C/C_0 ratio; C: the TMA concentration after EB irradiation, C_0: the initial concentration of TMA) concentrations under the N_2, O_2, and air background gases decreased as absorbed dose increased. And, TMA concentrations also declined continuously in the case of He background gas. However, TMA decomposition efficiency was lower (43 %, 10 kGy) when He was used as the background gas compared to

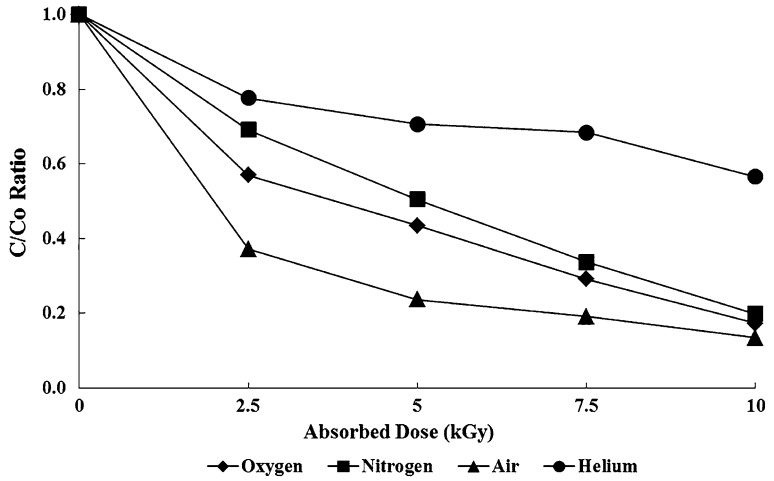

Fig. 1 Variations in trimethylamine decomposition ratio depending on the background gas

efficiency when the other background gases were used. The reason for this low removal efficiency was that He is a relatively stable molecule. On the other hand, the air background gas showed a maximum TMA removal efficiency of 86 % at 10 kGy, where 1 kGy based on air gas is equal to 1.291 J/L at 0 °C and 1 atm. (1 kGy based on He = 0.179 J/L at 0 °C and 1 atm.). TMA decomposition efficiencies under the N_2 and O_2 background gases were 80 and 82 % under the same absorbed dose condition, respectively.

It is reported that various radical species was generated by an EB irradiation [16] and those species affect decomposition processes of compounds. In the TMA decomposition reaction, when N_2 was used as a background gas, efficiencies could be increased approximately 35 % by N radicals such as N_2^*, $N(^2D)$, $N(^2P)$, $N(^4S)$, N_2^+ and N^+. Besides, at O_2 background gas, O radicals (O_2^*, $O(^3P)$, $O(^1D)$, O^+, O* and O_2^+) formed by the primary electron attack could strengthen approximately 37 % the decomposition effect of TMA.

This result indicates that the decomposition rate due to reactive species such as free radicals and ozone was higher than that by the primary electrons formed by EB irradiation. Such results were similar to the removal characteristics of other odorous volatile organic compounds [5, 12, 13].

Furthermore, the EB process can be applied to increase TMA decomposition efficiency without the need for an air supply at the actual site, because removal efficiency was highest when air was the background gas.

Figure 2 shows the G-values, which are an important determining factor for EB technology. The G-value is the number of atoms and molecules formed or decomposed when 100 eV energy is absorbed and used to assess the economic decomposition efficiency of pollutants when the EB was irradiated [13]. Hence, it means that pollutants are more decomposed as the G-value, which is a decomposition quantity by input energy, increases. The equation of G-value is depicted as follows:

$$G - value\left(\frac{\text{molecules}}{100\text{ eV}}\right) = 9.648 \times 10^6 \times \frac{Chemical\,yield\left(\frac{\text{mole}}{\text{kg}}\right)}{Absorbed\,dose(\text{kGy})}$$

The G-value decreased when absorbed doses increased, indicating that energy efficiencies were higher when the absorbed dose was lower (e.g., 2.5 kGy) from the

perspective of energy efficiency, because variances in removal efficiencies per unit energy were small when the TMA removal efficiencies reached a critical point. The G-value was lower for He than those of the other background gases because the removal efficiency per absorbed energy was low. This result was similar to those of previous studies of odorous compounds such as toluene, ethylbenzene, styrene, and *o*-xylene [10, 11, 13, 17, 18]

Initial Concentrations

The initial TMA concentration was diluted to 50, 100, and 200 ppm and irradiated using the EB to confirm TMA decomposition characteristics. Air was used as the background gas to ensure conditions similar to those used in industry. The EB (2.5–10 kGy) was irradiated based on the absorbed dose, and Fig. 3 shows the TMA removal efficiencies depending on the initial concentration. The TMA degradation rates increased as the absorbed dose increased and initial concentration decreased. The 50 and 100 ppm TMA treatment efficiencies at 2.5 kGy were >80 % and those at 10 kGy were >90 %. Additionally, residual rates of 200 ppm TMA decreased continuously when the absorbed dose increased, and removal efficiency at 10 kGy was approximately 86 %. As a result, the decomposition efficiencies of all initial TMA concentrations at a 10 kGy absorbed dose were approximately >90 %.

Figure 4 shows variations in the G-value depending on the initial concentration. When the absorbed dose was 2.5 kGy, the 50 and 100 ppm TMA removal efficiencies were very similar at 85 and 83 %, respectively. However, TMA decomposition rates per input energy under the same conditions were significantly different in terms of G-values. The G-values at a low initial concentration were relatively higher than those at a high initial concentration. When the G-value increased at the same absorbed dose, it means that removal efficiencies per input energy were more effective. However, at different initial conditions, the G-value at a high initial concentration would appear at a significantly higher dose, which was not necessarily related to removal efficiency as the absolute number of atoms and molecules formed or decomposed per some input energy was estimated regardless of initial concentration. Consequently, although the G-value was higher, actual decomposition efficiencies were lower. It is important to determine operating conditions based on the relationship between the G-value and removal efficiency.

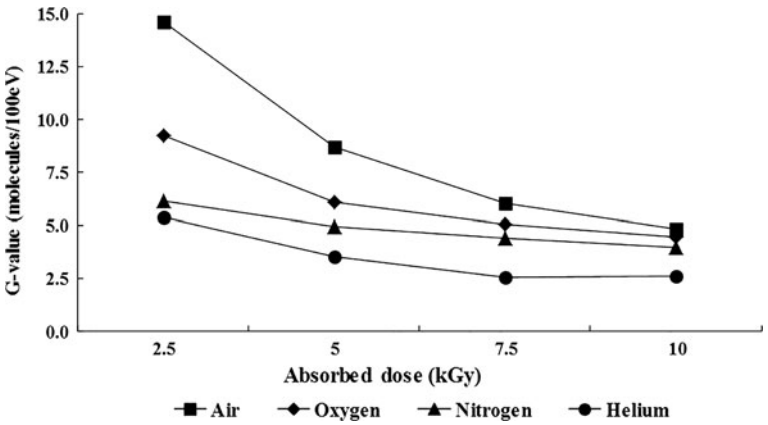

Fig. 2 Variations in the G-value depending on the background gas

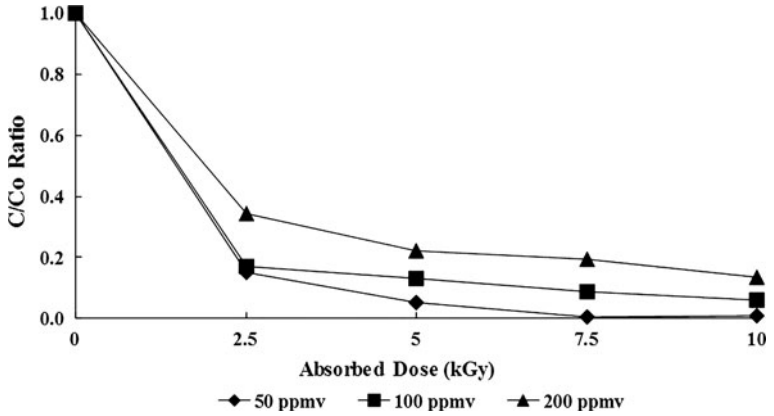

Fig. 3 Trimethylamine decomposition ratio based on initial concentration

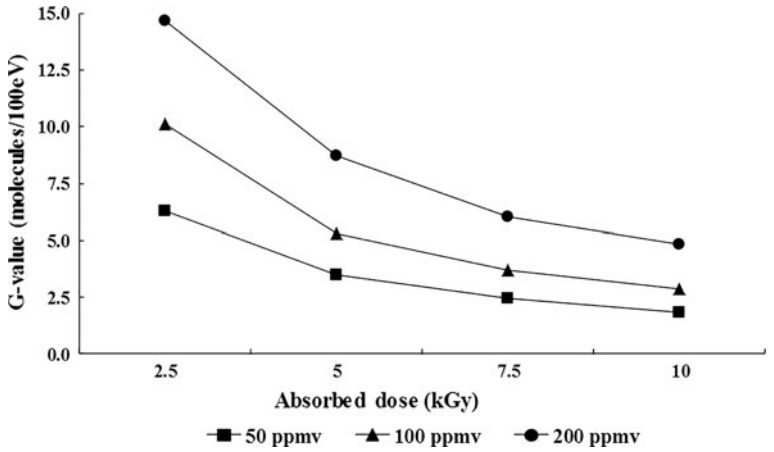

Fig. 4 Variations in the G-value based on initial trimethylamine concentration

Water Content

The OH radical induced by water vapor plays a pivotal role in the decomposition process of odorous compounds when using an EB [5, 8, 10, 13, 17]. In this study, the concentrations of water in air background gas were adjusted to approximately 1,200, 14,300 and 27,500 ppm in the batch reactors and irradiated with the EB to understand TMA (200 ppm) removal characteristics by the OH radical. As a result, the removal efficiency at a water content of 27,500 ppm increased to 10 % compared to that at a water content of 1,200 ppm when the absorbed dose was 2.5 kGy. Taken together, removal efficiencies increased from 5 to 30 % as water vapor increased.

The OH radical is one of the strongest active species generated by an EB and dominantly reacts with various air pollutants. The rate constant of the OH radical (6.11×10^{-11} cm^3 $molecule^{-1}$ s^{-1}) in the case of TMA is higher than those of O radical (2.18×10^{-11} cm^3 $molecule^{-1}$ s^{-1}), $O_2(^1\Delta_g)$ (4.98×10^{-15} cm^3 $molecule^{-1}$ s^{-1}), and O_3 (7.84×10^{-18} cm^3 $molecule^{-1}$ s^{-1}), Therefore, it suggests that the effect of the OH

radical should not be ignored in an EB control system [19–22]. TMA decomposition mechanism by OH radical is expected as following reactions [23];

$$OH^{\cdot} + (CH_3)_3N \rightarrow (CH_3)_2NCH_2^{\cdot} + H_2O \quad (1)$$

$$OH^{\cdot} + (CH_3)_3N \rightarrow (CH_3)_3N^{+\cdot} + OH^{-} \quad (2)$$

.

When adsorption and oxidation treatment systems are used for odorous compounds, the presence of water in the emissions may occasionally induce negative effects [24]. However, the removal efficiency of TMA using the EB process would increase as the amount of OH radicals and water content increased.

Continuous Flow System

A continuous flow test was conducted to confirm the applicability of actual industrial processes. Figure 5 shows the TMA decomposition efficiencies in a continuous flow system.

The decomposition efficiencies in the continuous flow reactor were similar to those in the batch reactor. The residual ratio decreased when the initial TMA concentration decreased and the absorbed dose increased. The removal efficiency of 50 ppm TMA was >99 % at 10 kGy, and those at 100 and 200 ppm TMA were 81 and 67 %, respectively, at the same absorbed dose. Removal efficiencies in the continuous flow reactor were lower than those in batch reactor, indicating that the conversion of EB energy was insufficient because of the cavitation phenomenon that occurs due to reactor turbulence.

On the other hand, GC/MSD (Agilent 5975, USA) was used to identify by-products formed by TMA decomposition using EB. As results of quality analysis, residues TMA and trace CH_4 were observed. And, the concentrations of CH_4 would also be slightly increased when the degraded TMA amount was increased. No studies on gaseous TMA decomposition mechanism using an EB have been reported. However, the mechanism would be expected through previous studies. Deac et al. [25] reported TMA would be a low energy source for the production of the production of CH_3 radicals because the activation energy of the H_3C–N bond cleavage is to have a value of 51–52 kcal/mol, while the same energy for the C–C bond is between 81 and 71 kcal/mol. And, they reported that generated CH_3

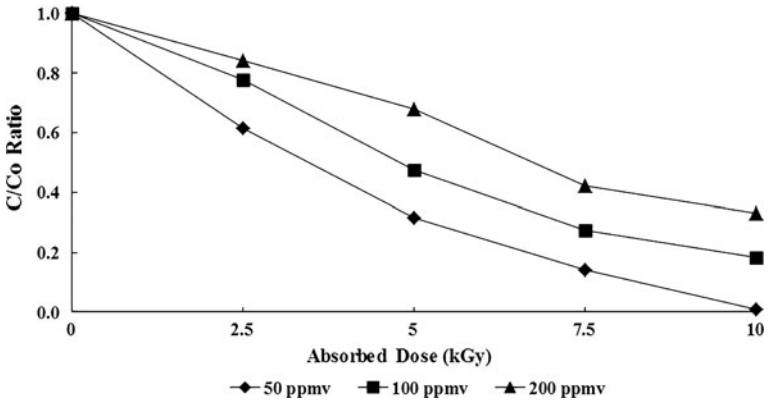

Fig. 5 Trimethylamine decomposition ratios in a continuous flow system

radicals react with hydrogen to produce CH_4 in infrared multiphoton dissociation of TMA. Also, Kozak and Gesser [26] reported that CH_4 was formed by CH_3 radical react with TMA in the photolysis reaction. A similar result was found by Bamford and Gesser et al. [27–30].

Through results by quality analysis in this study and by previous reported studies, several possibilities of CH_4 generated from TMA decomposition were considered. The first step is that CH_3 radicals were formed by the electron attack and it is expected as following reactions.

$$(CH_3)_3N \rightarrow (CH_3)_2N + CH_3 \quad (3)$$

$$\rightarrow CH_3NCH_2 + H + CH_3 \quad (4)$$

$$\rightarrow NC_2H_4 + H_2 + CH_3 \quad (5)$$

.

Then $(CH_3)_2N$ was converted into $(CH_3)_2NH$ and CH_3NCH_2 by reaction (6) [31]. In this reaction, some $(CH_3)_2NH$ were came back $(CH_3)_2N$ as reported by Bamford [27]. And, CH_3NCH_2 was also produced by $(CH_3)_2N$ react with residual O_2 [32].

$$2(CH_3)_2N \rightarrow (CH_3)_2NH + CH_3NCH_2 \quad k = 3.32 \times 10^{-12}\ cm^3\ molecule^{-1}\ s^{-1} \quad (6)$$

$$O_2 + (CH_3)_2N \rightarrow CH_2{=}NCH_3 + HO_2 \quad k = 1.48 \times 10^{-6}\ cm^3\ molecule^{-1}\ s^{-1} \quad (7)$$

The second step is that CH_3 radicals were converted into CH_4 by reaction with H, $(CH_3)_2NH$, $(CH_3)_2N$ and residual TMA as follows [31, 33–35];

$$(CH_3)_3N + CH_3 \rightarrow (CH_3)_2NCH_2 + CH_4 \quad k = 2.54 \times 10^{-24}\ cm^3\ molecule^{-1}\ s^{-1} \quad (8)$$

$$(CH_3)_2NH + CH_3 \rightarrow (CH_3)_2N + CH_4 \quad k = 2.13 \times 10^{-18}\ cm^3\ molecule^{-1}\ s^{-1} \quad (9)$$

$$(CH_3)_2N + CH_3 \rightarrow CH_3NCH_2 + CH_4 \quad k = 1.31 \times 10^{-11}\ cm^3\ molecule^{-1}\ s^{-1} \quad (10)$$

$$H + CH_3 \rightarrow CH_4 \quad k = 2.04 \times 10^{-10}\ cm^3\ molecule^{-1}\ s^{-1} \quad (11)$$

Also, in whole reaction processes, it is expected that C_2H_2, C_2H_4, C_2H_6, $(CH_3)_2NH$, $CH_2(OH)_2$ and heavy compounds such as $(CH_3)_2N\text{-}CH_2\text{-}N(CH_3)_2$ and $(CH_3)_2NCH_2\text{-}C{\equiv}N$ were generated [27, 29]. However, we could not find those compounds in this experiment.

CO/CO_2 Formation

The amounts of generated CO and CO_2 determine the efficiency of air pollution control systems [36]. The concentrations formed after EB irradiation in the continuous flow system were continuously measured, and CO concentrations increased as the absorbed dose and/or initial TMA concentration increased (Fig. 6). This means that the CO concentration increased due to incomplete combustion in the reactor. Additionally, the CO concentrations observed at 200 ppm TMA, which contained more carbon atoms than that of other TMA concentrations, was relatively higher than those at 100 and 50 ppm TMA.

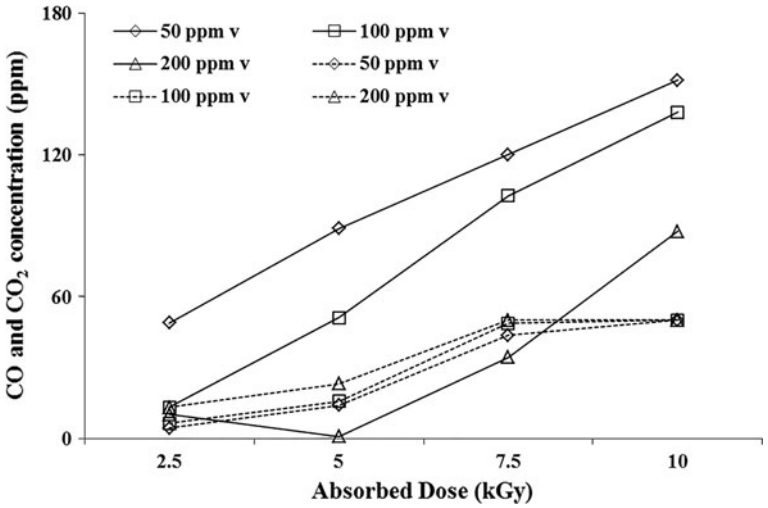

Fig. 6 CO and CO_2 concentrations based on absorbed dose (*Dotted lines* CO; *Solid lines* CO_2)

The CO_2 concentration range measured after EB irradiation was approximately 0–150 ppm and rose as absorbed dose increased (Fig. 6). Additionally, CO_2 concentrations at 200 ppm TMA were 30–80 ppm lower than those at 50 ppm TMA. Similar results were discovered following butane and styrene treatment by EB irradiation [11, 13]. And, the CO and CO_2 concentration range formed by EB irradiation varied according to the compound.

We confirmed that CO and CO_2 concentrations rose as absorbed dose increased. This study was conducted at comparatively high concentrations (50–200 ppm) to decidedly understand removal efficiency based on initial concentration. When considering the decomposition efficiency, energy efficiency (G-value), and emission concentration generated from actual industrial facilities, the EB treatment would be useful for an effective operation because removal efficiency was high and the amounts of CO and CO_2 formed were significantly lower at 2.5 kGy. However, a more in-depth study about CO and CO_2 should be conducted.

Conclusions

This study was carried out to understand the influence of various factors, including initial concentration, background gas, absorbed dose, and reactor type on TMA decomposition characteristics. The results are as follows:

- Radicals had a greater influence on TMA decomposition than primary electrons.
- Removal efficiencies increased from 5 to 30 % as water vapor increased.
- The decomposition efficiency at 10 kGy was approximately 99 % in the continuous flow system when the initial TMA concentration was 50 ppm.
- CH_3 radical formed by EB irradiation was converted into CH_4 by reaction with H, $(CH_3)_2NH$, and residual TMA.

Although, this study was conducted at relatively high TMA concentrations (50–200 ppm), it was confirmed that the EB had good TMA treatment efficiency. This

means that an EB can be applied to TMA treatment at a low concentration and a high flow rate. It would be possible to develop a more efficient control system by combining EB with other control technologies. Odors emitted from industrial facilities are composed of not only TMA but a variety of odorous compounds. Therefore, a mechanistic study should be conducted in the future. A more appropriate EB treatment technology must be studied based on an actual field investigation.

Acknowledgments This study was supported by the Basic Science Research Program through the National Research Foundation of Korea (NRF) funded by the Ministry of Education, Science, and Technology (2012R1A6A3A03039668). This study was also supported by the Korean Ministry of Environment as part of "The Eco-Technopia 21 Project".

References

1. Kabir E, Kim KH (2010) An on-line analysis of 7 odorous volatile organic compounds in the ambient air surrounding a large industrial complex. Atmos Environ 44:3492–3502
2. Ding Y, Shi JY, Wu WX, Yin J, Chen YX (2007) Trimethylamine (TMA) biofiltration and transformation in biofilters. J Hazard Mater 143:341–348
3. US EPA (2008) Acute exposure guideline levels (AEGLs) for trimethylamine (CAS Reg. No. 75-50-3)
4. Chang MB, Tseng TD (1996) Gas-phase removal of H_2S and NH_3 with dielectric barrier discharges. J Environ Eng 122:41–46
5. Son YS, Kim KJ, Kim JC (2010) A review on VOCs control technology using electron beam. AJAE 4:63–71
6. Xia L, Huang L, Shu X, Zhang R, Dong W, Hou H (2008) Removal of ammonia from gas stream with dielectric barrier discharge plasma. J Hazard Mater 152:113–119
7. Kim NJ, Sugano Y, Hirai M, Shoda M (2000) Removal of a high load of ammonia gas by a marine bacterium, *Vibrio alginolyticus*. J Biosci Bioeng 90:410–415
8. Chaichanawong J, Tanthapanichakoon W, Charinpanitkul T, Eiad-ua A, Sano N, Tamon H (2005) High-temperature simultaneous removal of acetaldehyde and ammonia gases using corona discharge. Sci Technol Adv Mater 6:319–324
9. Tanthapanichakoon W, Charinpanitkul T, Chaiyo S, Dhattavorn N, Chaichanawoug J, Sano N, Tamon H (2004) Effect of oxygen and water vapor on the removal of styrene and ammonia from nitrogen by non-pulse corona-discharge at elevated temperatures. Chem Eng J 97:213–223
10. Kim JC (2002) Factors affecting aromatic VOC removal by electron beam treatment. Radiat Phys Chem 65:429–435
11. Son YS, Park KN, Kim JC (2010) Control factors and by-products during decomposition of butane in electron beam irradiation. Radiat Phys Chem 79:1255–1258
12. Hirota K, Hakoda T, Arai H, Hashimoto S (2002) Electron-beam decomposition of vaporized VOCs in air. Radiat Phys Chem 65:415–421
13. Son YS, Son YS, Park JH, Kim P, Kim JC (2012) Oxidation of gaseous styrene by electron beam irradiation. Radiat Phys Chem 81:686–692
14. Sun Y, Chmielewski AG, Bulka S, Zimek Z (2006) Influence of base gas mixture on decomposition of 1,4-dichlorobenzene in an electron beam generated plasma reactor. Plasma Chem Plasma Process 26:347–359
15. Chmielewski AG (2007) Industrial applications of electron beam flue gas treatment-from laboratory to the practice. Radiat Phys Chem 76:1480–1484
16. Mätzing H (1991) Chemical kinetics of flue gas cleaning by irradiation with electrons. In: Prigogine I, Rice SA (eds) Advances in chemical physics, vol LXXX. Wiley, New York, pp 315–402
17. Kim KJ, Kim JH, Son YS, Chung SG, Kim JC (2012) Advanced oxidation of aromatic VOCs using a pilot system with electron beam-catalyst coupling. Radiat Phys Chem 81:561–565
18. Son YS, Kim KJ, Kim JC (2010) Comparison of the decomposition characteristics of aromatic VOCs using an electron beam hybrid system. Radiat Phy Chem 79:1270–1274
19. Atkinson R, Pitts JN (1978) Kinetics of the reactions of $O(^3P)$ atoms with the amines CH_3NH_2, $C_2H_5NH_2$, $(CH_3)_2NH$, and $(CH_3)_3N$ over the temperature range 298–440°K. J Chem Phy 68:911–915
20. Tuazon EC, Atkinson R, Aschmann SM, Arey J (1994) Kinetics and products of the gas-phase reactions of O_3 with amines and related compounds. Res Chem Intermed 20:303–320

21. Ogryzlo EA, Tang CW (1970) Quenching of oxygen (1Σg) by amines. J Am Chem Soc 92:5034–5036
22. Atkinson R, Perry RA, Pitts JN (1978) Rate constants for the reactions of the OH radical with $(CH_3)_2NH$, $(CH_3)_3N$, and $C_2H_5NH_2$ over the temperature range 298–426°K. J Chem Phys 68: 1850–1853
23. Das S, Schuchmann MN, Schuchmann H-P, Sonntag CV (1987) The production of the superoxide radical anion by the OH radical-induced oxidation of trimethylamine in oxygenated aqueous solution. The kinetics of the hydrolysis of (hydroxymethyl) dimethylamine. Chem Ber 120:319–323
24. Schlegelmilch M, Streese J, Steqmann R (2005) Odour management and treatment technologies: an overview. Waste Manag 25:928–939
25. Deac I, Almasan V, Palibroda N, Indrea E, Filip X, Ursu I (1996) A low energy source for production of CH_3, CN and other free radical: IRMPD of di and trimethylamine molecules. Appl Surf Sci 106: 223–227
26. Kozok PJ, Gesser H (1960) The photolysis of triethylamine, and reactions of methyl radicals with triethylamine and diethylamine. J Chem Soc (resumed) 448–452. doi:10.1039/JR9600000448
27. Bamford CH (1939) A study of the photolysis of organic nitrogen compounds. Part I. Dimethyl- and diethyl-nitrosoamines. J Chem Soc (resumed) 12–17. doi:10.1039/JR9390000012
28. Bamford CH (1939) A study of the photolysis of organic nitrogen compounds. Part II. Aliphatic amines. J Chem Soc (resumed) 17–26. doi:10.1039/JR9390000017
29. Gesser H, Mullhaupt JT, Griffiths JE (1957) The photolysis of trimethylamine. J Am Chem Soc 79:4834–4836
30. Seetula J, Blomqvist K, Kalliorinne K, Koskikallio J (1985) Kinetics of reactions between CH_3, CH_3CO and $(CH_3)_2N$ radicals produced by flash-photolysis of N, N-dimethylacetamide in gas-phase. Finn Chem Lett 69:139–140
31. Seetula J, Blomquist K, Kalliorinne K, Koskikallio J (1986) Kinetics of radical reactions between methyl, acetyl and dimethylamino radicals formed in the flash photolysis of N, N-dimethylacetamide in the gas phase. Acta Chem Scand 40:658–663
32. Lindley CRC, Calvert JG, Shaw JH (1979) Rate studies of the reactions of the $(CH_3)_2N$ Radical with O_2, NO, and NO_2. Chem Phys Lett 67:57–62
33. Gray P, Jones A, Thynne JCJ (1965) Kinetics and sites of methyl radical attack on dimethylamine and deuterated dimethylamine. Trans Faraday Soc 61:474–483
34. Tsang W (1989) Rate constants for the decomposition and formation of simple alkanes over extended temperature and pressure ranges. Combust Flame 78:71–86
35. Edwards DA, Kerr JA, Lloyd AC, Trotman-Dickenson AF et al (1966) Hydrogen-abstraction reactions by methyl radicals from nitrogen-containing compounds. J Chem Soc A 621–622. doi:10.1039/J19660000621
36. Anderson KM, Ou D, Wu YB, Jajeh A, Harris JE (1999) Induction of type 1 programmed cell death in U937 cells by the antioxidant, butylated hydroxy-toluene or the free radical spin trap, NTBN. Leuk Res 23:665–673